# Direct visualization by electron microscopy of the weakly bound intermediates in the actomyosin adenosine triphosphatase cycle

Thomas D. Pollard,* Dhansukhlal Bhandari,* Pamela Maupin,* Daniel Wachsstock,* Alan G. Weeds,‡ and Henry G. Zot*

*Department of Cell Biology and Anatomy, The Johns Hopkins Medical School, Baltimore, Maryland 21205 USA; and ‡Medical Research Council Laboratory of Molecular Biology, Cambridge, UK

ABSTRACT We used a novel stopped-flow/rapid-freezing machine to prepare the transient intermediates in the actin-myosin adenosine triphosphatase (ATPase) cycle for direct observation by electron microscopy. We focused on the low affinity complexes of myosin-adenosine triphosphate (ATP) and myosin-adenosine diphosphate (ADP)-$P_i$ with actin filaments since the transition from these states to the high affinity actin-myosin-ADP and actin-myosin states is postulated to generate the molecular motion that drives muscle contraction and other types of cellular movements. After rapid freezing and metal replication of mixtures of myosin subfragment-1, actin filaments, and ATP, the structure of the weakly bound intermediates is indistinguishable from nucleotide-free rigor complexes. In particular, the average angle of attachment of the myosin head to the actin filament is ~40° in both cases. At all stages in the ATPase cycle, the configuration of most of the myosin heads bound to actin filaments is similar, and the part of the myosin head preserved in freeze-fracture replicas does not tilt by more than a few degrees during the transition from the low affinity to high affinity states. In contrast, myosin heads chemically cross-linked to actin filaments differ in their attachment angles from ordered at 40° without ATP to nearly random in the presence of ATP when viewed by negative staining (Craig, R., L. E. Greene, and E. Eisenberg. 1985. *Proc. Natl. Acad. Sci. USA.* 82:3247–3251, and confirmed here), freezing in vitreous ice (Applegate, D., and P. Flicker. 1987. *J. Biol. Chem.* 262:6856–6863), and in replicas of rapidly frozen samples. This suggests that many of the cross-linked heads in these preparations are dissociated from but tethered to the actin filaments in the presence of ATP. These observations suggest that the molecular motion produced by myosin and actin takes place within the myosin head at a point some distance from the actin binding site or does not involve a large change in the shape of the myosin head.

## INTRODUCTION

The molecular mechanics that produce force and motion during the interaction of actin, myosin, and adenosine triphosphate (ATP) have been difficult to study, because the myosin heads that comprise the active part of the crossbridges between the two sliding filaments act asynchronously as shown originally by Huxley and Brown (1967). On the other hand, we now understand the chemistry, kinetics, and energetics of the cyclic interaction of myosin, actin, and ATP in detail (reviewed in Hibberd and Trentham, 1986; Geeves, 1991; Taylor, 1992). These biochemical insights, summarized in a highly simplified scheme in Fig. 1, provide the foundation from which we can work to establish the molecular mechanics. For the present purposes, there are three essential features of this mechanism.

First, in the absence of nucleotides, myosin heads (M) bind to actin filaments (A) with very high affinity ($K_d < 10^{-9}$ M). This has made it possible to document the structure of the AM complex by electron microscopy (Huxley, 1963; Moore et al., 1970; Taylor and Amos, 1981; Toyashima and Wakabayashi, 1985; Milligan and Flicker, 1987; Tokunaga et al., 1987). These "rigor" complexes have the appearance of polarized arrowheads that repeat every 36 nm as determined by the helical structure of the actin filament. Each myosin head binds to a single actin subunit with its long axis tilted and slewed relative to the long axis of the actin polymer. The structure of the AMD complex (actomyosin with adenosine diphosphate [ADP] in the active site) is similar to the AM complex (Craig et al., 1985).

Second, myosin binds and hydrolyzes ATP rapidly, but the products, ADP and inorganic phosphate (P), dissociate very slowly unless stimulated by the presence of actin filaments (Lymn and Taylor, 1971). The 200-fold higher rate of product dissociation when MDP is bound to an actin filament accounts for the actin-activation of the myosin adenosine triphosphatase (ATPase) activity observed at steady state (Eisenberg and Moos, 1968). However, when ATP or the products occupy the active site on the myosin head, the affinity of the head for actin filaments is reduced by four or five orders of magnitude (Stein et al., 1984). The $K_d$s of the AMT and AMDP complexes are on the order of $10^{-5}$ to $10^{-4}$ M, depending on the ionic conditions, and the individual heads bind to and dissociate from actin filaments at rates that far exceed the rate of the overall ATPase cycle. Furthermore, new physiological evidence suggests that the force producing states also bind to and dissociate from actin filaments multiple times during one cycle of ATP hydrolysis (Brenner, 1991; Lombardi et al., 1992).

Third, the large free energy change during the dissociation of the products from the myosin (White and Taylor, 1976) is generally assumed to be coupled to structural changes in the myosin-actin complex that produce force and motion. Since isolated myosin heads obtained by proteolytic digestion (subfragment-1 or S1) can move

D. Bhandari's present address is FMBRA, Herts, UK.

H. Zot's present address is Department of Physiology, University of Texas, Southwestern Medical Center, Dallas, TX 75325.



0006-3495/93/02/454/18 $2.00

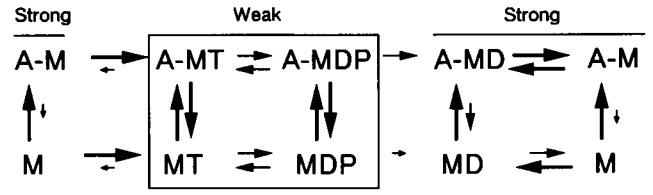


FIGURE 1 A highly simplified actomyosin ATPase mechanism. *A*, filamentous actin; *M*, myosin head; *T*, ATP; *D*, ADP; *P*, inorganic phosphate. The arrows indicate the approximate relative values of the rate constants. Myosin in the AM and AMD states are considered to be strongly bound to actin filaments because the dissociation rate constants are small. Myosin in the AMT and AMDP states is considered to be weakly bound to actin filaments because the dissociation rate constants are large, leading to a rapid equilibrium between bound and free myosin. The objective of this study was to compare the structure of the weakly bound intermediates (shown in the box) with the tightly bound, rigor complex, AM.

actin filaments (Toyoshima et al., 1987) and produce force (Kishino and Yanagida, 1988), the structural changes are likely to be in the myosin head itself or at the interface between the myosin and actin molecules.

For more than two decades it has been believed widely that the sliding movement of an actin filament relative to myosin is the direct consequence of a change in the shape of either the complex of S1 and actin or the myosin S1 itself that occurs once per ATPase cycle. The most widely considered model has the myosin head tilting on the surface of the actin filament from an angle of 90° for AMDP to 45° for AMD and AM (Huxley, 1969). A wealth of physiological data support the idea that the mechanical step associated with the hydrolysis of each ATP is ~5–10 nm, a size that could be accommodated by a tilting crossbridge mechanism (reviewed in Huxley and Kress, 1985). These models predict large differences in the structures of AMDP and AMD and have provided a challenge for structural studies to establish the location of the hypothesized molecular motion.

Many biophysicists have sought the molecular motion in the actomyosin system that is hypothesized by the standard crossbridge models without resolution of the problem (see reviews in Thomas, 1987; Cooke, 1990). In particular, there is no strong evidence for 90° states. For example, by electron microscopy, myosin heads covalently cross-linked to actin filaments are attached at 45° in the absence of ATP but are disordered, rather than attached uniformly at 90°, in the presence of ATP (Craig et al., 1985; Applegate and Flicker, 1987). Further questions have been raised by new experiments on the size of the translation of an actin filament per ATP hydrolyzed by myosin. Some (Harada et al., 1990) but not all (Uyeda et al., 1991) of the work suggests steps much larger than accomodated by a single cycle of a tilting crossbridge. New mechanical data also argue for multiple force-producing steps per ATP hydrolyzed (Brenner, 1991; Lombardi et al., 1992). This work has led to the reconsideration of mechanisms that do not involve wholesale structural changes in the actin-myosin complex (Vale and Oosawa, 1990). On the other hand, none of the evidence rules out discrete steps produced by conformational changes in the actin-myosin complex.

We have reinvestigated the problem with the hope that the unique ability of electron microscopy to visualize individual molecules would provide information on the orientation of the myosin head at various steps in the ATPase cycle. Specifically, we sought direct evidence for the 90° orientation proposed in the most popular crossbridge models. We used rapid mixing, rapid freezing, and freeze-fracturing to obtain millisecond time resolution and to enable us to work with high enough concentrations of protein to allow mass action to drive substantial numbers of low affinity myosin-nucleotide intermediates onto the actin filaments. We found that the weakly bound myosin-nucleotide intermediates attach to actin filaments at an angle of ~40°, similar to the rigor complexes without ATP. In contrast, when S1 is chemically cross-linked to actin filaments, its orientation is nearly random in the presence of ATP, suggesting that many of these heads are dissociated but tethered to the actin filaments. These results provide new evidence that translocation of myosin relative to actin occurs by relatively small conformational changes rather than tilting of the whole myosin head on the surface of the actin filament. Any large molecular motions in the complex may occur within the myosin head some distance from its binding site on the actin filament, near the junction of the head with the tail.

## MATERIALS AND METHODS

### Reagents

ATP and dithiothreitol were purchased from Sigma Chemical Corp. (St. Louis, MO). Other chemicals were reagent grade.

### Proteins

Myosin was purified from rabbit back and leg muscles (Kielley and Harrington, 1959) and digested with chymotrypsin to yield the head fragment called S1 (Weeds and Taylor, 1975). For comparison, S1 was also produced by digestion with papain (Lowey et al., 1969). Actin was purified from an acetone powder of rabbit muscle (Eisenberg and Kielley, 1974). S1 was chemically cross-linked to actin filaments with 1-ethyl-3-(3-dimethylaminopropyl)-carbodiimide (EDC) and freed of uncross-linked S1 as described by Mornet et al. (1981). S1, actin filaments, and cross-linked acto-S1 were dialyzed overnight against 1 mM $MgCl_2$, 0.5 mM dithiothreitol, 5 mM ammonium carbonate (pH 8.5). Immediately before the experiments, methanol was added to S1 at 0°C in small increments to a concentration of 10%. The methanol was included to improve the freezing and freeze fracturing (Heuser and Kirschner, 1980).

### Biochemical assays

The concentrations of the proteins were determined by absorption using extinction coefficients of 0.62 $cm^2mg^{-1}$ at 290 nm for actin and

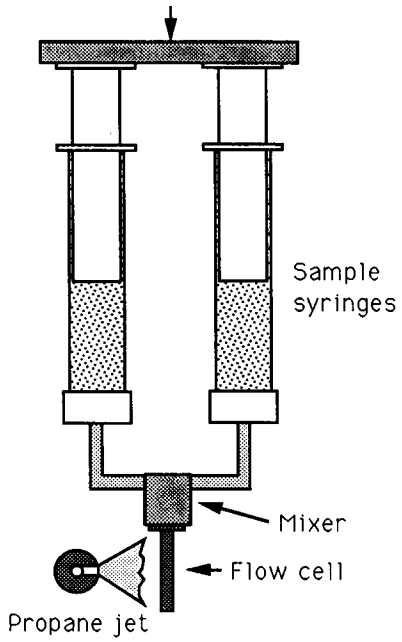


FIGURE 2 Schematic drawing of the mixing and freezing unit. Myosin heads (S1) in one syringe are mixed with actin filaments and ATP in the other syringe and injected (after ~3 ms) into a thin-walled copper flow cell. After a preset delay of 1–2,500 ms, the contents of the flow cell are rapidly frozen with a jet of liquid propane cooled to −190°C. The frozen sample is then prepared for electron microscopy by freeze fracturing and replication of the surface with platinum and carbon. Details can be found in Pollard et al. (1990).

0.65 $cm^2mg^{-1}$ at 280 nm for myosin S1. Steady-state ATPase activities were measured at 25°C in the protein dialysis buffer. Inorganic phosphate was measure colorimetrically (Pollard and Korn, 1973).

## Stopped flow kinetics

The time course of ATP hydrolysis and binding of actin and S1 were followed by 90° scattering of 365 nm light in a stopped-flow unit (Johnson, 1986). The dead time is 3.5 ms (Sinard and Pollard, 1990).

## Stopped flow/rapid freezing

Preparation of samples for freeze fracturing was done with a prototype machine designed by Pollard et al. (1990). This device has the same geometry and mixer as the stopped-flow spectrophotometer, except that the sample is injected into a 1.5 × 10-mm cylindrical copper flow cell with walls 10 μm thick (Fig. 2). The sample syringes and mixer were thermostated at 25°C. The flow cell was at room temperature until it was lowered into the ready position near the nozzle of the freezing jet ~1 s before freezing. The flow cell was brought to 25°C by injection of ~200 μl of sample before stopping the flow and beginning the aging before freezing. After a preset delay of 1 ms to 10 s, the contents of the flow cell were rapidly frozen with a high-pressure jet of liquid propane at a temperature of −190°C. Theoretical estimates predict that the superficial layers are frozen in <1 ms (Kopstad and Elgsaeter, 1982). The frozen flow cell was transferred to the cold stage of a freeze-fracture machine (Balzers, Hudson, NH). Under vacuum, a thin tangential strip of the flow cell was cut away to expose the frozen specimen. The surface layer of ice was then sublimed at −106°C for 4 min to expose the filaments. The surface of the specimen was rotary replicated with platinum and reinforced with carbon. The replica was recovered and viewed in a conventional transmission electron microscope at a magnification of ~50,000×.

## Data collection and analysis

The replicas were searched for areas with well-frozen and replicated actin filaments according to the criteria given in Results. Between 10 and 40 fields were photographed from each specimen. Negatives from a variety of specimens were mixed together randomly and projected at a final magnification of ~500,000× in a photographic enlarger. Three different authors examined these images in a blinded fashion, tracing the path of each actin filament on paper and marking the presence of all particles attached to the filaments. Due to its uniform size, S1 was relatively easy to distinguish from debris. The azimuthal angle of attachment of individual S1s was apparent in the replicas, so that those S1s bound to the sides of the filaments could be selected for measurement of their axial angle of attachment to the filament. These angles were marked and later measured with a protractor.

The polarity of each filament was assigned based on the orientation of the majority of the heads. Filaments with only one or two heads were excluded as ambiguous. After the measurement of attachment angles and the assignment of polarity, the identity of the micrographs was revealed so the data from each sample could be pooled. The attachment angles were grouped in 10° intervals and displayed in histograms or graphs with polar coordinates.

In cases where many heads with uniform polarity were attached to a filament, the assignment of polarity was obvious, but when the orientations of the heads were highly variable (such as cross-linked acto-S1 in ATP), the assignment of polarity was subject to error. To determine how our "majority wins" method of assigning filament polarity affects the observed distribution of attachment angles, we used elementary probability theory to calculate how the observed polarities depend on the actual bias in the orientation, the number of heads per filament, and the number of filaments observed.

If the probability that a given S1 head is oriented toward the pointed end of the actin filament is $\omega$, then the probability of $k$ heads toward the pointed end on a filament with $n$ heads is:

$$p(k, n; \omega) = \omega^k(1 - \omega)^{n-k}n!/k!(n - k)!.$$

This is the binomial distribution.

However, due to the way the filament polarities are assigned, if a filament has $k < n/2$, then the barbed end is incorrectly called the pointed end, and the filament is scored as having $n - k$ heads oriented toward the pointed end. In other words, the apparent probability distribution is:

$$\begin{aligned} p'(k, n; \omega) &= 0 && \text{if } k < n/2 \\ &= p(k, n; \omega) && \text{if } k = n/2 \\ &= p(k, n; \omega) + p(n - k, n; \omega) && \text{if } k > n/2 \end{aligned}$$

This formula can be integrated numerically over all the filaments measured to obtain the total probability distribution. A Macintosh program in C for this calculation is available from Daniel Wachsstock of the Johns Hopkins Medical School. For example, if $n_i$ is the number of heads on the $i$th filament, then the total probability distribution of the first $N$ filaments is $P(k, N; \omega)$. This is the probability of the first $N$ filaments having a total of $k$ heads oriented toward the pointed end. If $N = 1$, then there is only one filament and the probability distribution is that was calculated above:

$$P(k, 1; \omega) = p'(k, n_1; \omega).$$

For $N > 1$, the probability is the sum of the probability of all $k$ "pointed" heads being on the last filament and none of the $k$ being on the others, plus the probability of $k - 1$ heads on the last and 1 head oriented to the pointed end on the others, plus the probability of $k - 2$ heads on the last and 2 on the others, and so on. In other words:

$$P(k, N; \omega) = \sum_{i=0}^{k} p'(i, n_N; \omega) \cdot P(k - i, N - 1; \omega).$$

And when $N$ is equal to the total number of filaments, $P(k, N; \omega)$ is the probability distribution for all the filaments.

## RESULTS

### Experimental conditions and characterization of the proteins

All of the electron microscopy experiments reported here were carried out in a low ionic strength solution buffered with bicarbonate and containing 10% methanol. The methanol is used to reduce ice crystal formation during freezing, because it sublimes much like water at −106°C during the etching process (Heuser and Kirschner, 1980; Heuser, 1983). A low salt concentration is necessary to avoid deposition of nonvolatile material on the proteins during etching. Fortunately, much of the characterization of the actomyosin ATPase mechanism also has been carried out at low ionic strength (for example, see Stein et al., 1984).

Methanol activates the steady-state hydrolysis of ATP by S1 and actin filaments. Judging from the dependence of the ATPase activity as a function of the actin filament concentration, the $K_{ATPase}$ values were 6.5 $\mu$M without methanol and 8.0 $\mu$M with 10% methanol. The maximum velocity ($V_{max}$) was 11 $s^{-1}$ in buffer and 23 $s^{-1}$ in buffer with 10% methanol. Samples were prepared fresh daily, because some loss of ATPase activity was detected after 24 h in 10% methanol.

### Time course of ATP hydrolysis and binding of S1 to actin filaments

Light scattering of mixtures of actin filaments and S1 is approximately proportional to the extent of S1 binding to the filaments (White and Taylor, 1976), so that this method provided a quantitative measure of S1 binding during a stopped-flow experiment (Fig. 3). After mixing actin + ATP with S1 in the low ionic strength buffer, a steady-state level of binding was reached within the dead time of the machine. The extent of binding depended on the concentrations of both S1 and actin filaments approximately as described by others (Stein et al., 1984), although we did not attempt to repeat their work in enough detail to measure a binding constant. For example, in the experiment in Fig. 3, ~30% of the S1 bound to actin filaments at steady state in the presence of ATP. After a period of time that depended on the concentrations of the proteins and ATP, the ATP was consumed and the light scattering increased to a higher equilibrium level. The midpoint of this transition provided an independent measure of the steady-state acto-S1 ATPase rate that agreed with our colorimetric assays and published values for these conditions. Samples with 10% methanol gave the same results except that the ATPase rate was higher and the lag before rebinding of the S1 was shorter.

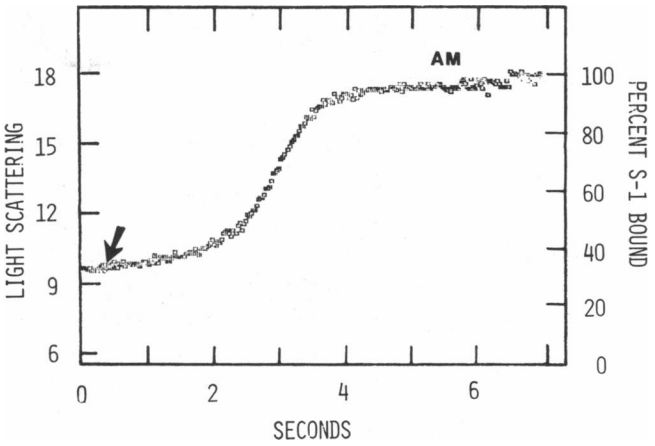


FIGURE 3 Time course of the reaction of S1 and actin with ATP. Actin filaments (80 $\mu$M) with 1.0 mM ATP were mixed 1:1 with 40 $\mu$M myosin S1 and 90° light scattering at 365 nm (in arbitrary units) followed with time. The final concentrations were 40 $\mu$M actin, 20 $\mu$M S1, 0.5 mM ATP, 2 mM imidazole (pH 7.1), 1 mM $MgCl_2$, 0.25 mM dithiothreitol. The light scattering increases when the ATP is consumed and all of the S1 binds to actin filaments. The fraction of S1 bound to the actin was estimated from the light scattering of rigor samples of actin with various mole ratios of S1. The steady-state ATPase estimated from the time for half maximal binding to actin was 8 $s^{-1}$. The samples for electron microscopy were taken during the phase of steady-state ATP hydrolysis when a small fraction of the S1 was bound to actin filaments, for example at 500 ms as indicated by the arrow. Very similar results were obtained in the methanol containing buffer used for rapid freezing.

We used this light-scattering data to establish the biochemical state of samples frozen for electron microscopy. For example, in the example in Fig. 3, samples taken at 50 ms would be expected to contain a mixture of S1-ATP and S1-ADP-$P_i$ in rapid equilibrium with actin filaments such that 30% of the myosin heads were bound to the actin at any given time. Similarly, a sample taken at 10 s would have 100% of the S1 bound tightly to the actin filaments.

### Electron microscopy of rapidly frozen specimens

We froze actin filaments under a wide variety of conditions and completed more than 400 freeze-fracture runs. We usually mixed 20–40 $\mu$M actin filaments containing 0–1 mM ATP with an equal volume of 0–40 $\mu$M S1. The delay between mixing and freezing varied from 3.5 ms (the dead time) to 10 s. The turbulence during mixing had no obvious effect on the actin filaments or their orientation, since they were randomly arranged in both static samples (Fig. 4) and samples frozen immediately after injection into the flow cell (Figs. 5 and 6). The density of actin filaments was high judging from the large number of filaments cross-fractured (Figs. 5 and 6) but only a few were parallel to the fracture face and visi-

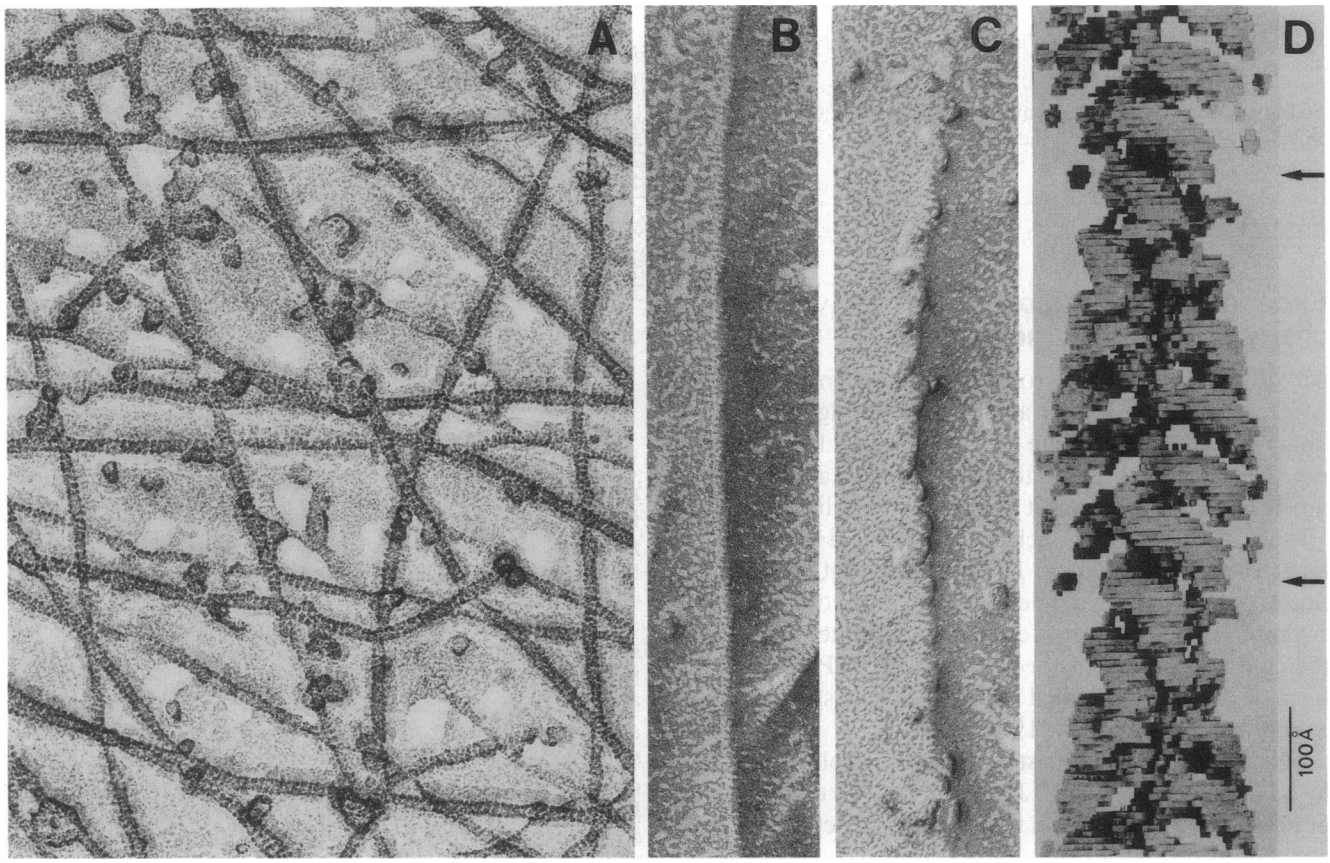


FIGURE 4 Electron micrographs of freeze-fracture replicas of (*A* and *B*) actin filaments alone and (*C*) rigor complexes of 2 $\mu$M S1 with 30 $\mu$M actin filaments compared with (*D*) a three-dimensional reconstruction of a decorated actin filament from the work of Toyoshima and Wakabayashi (1985). The sample in *A* was deeply etched, fully exposing the actin filaments. The samples in *B* and *C* were lightly etched, leaving the filaments partially embedded in the ice at the time of replication. The 5.5-nm repeat of the subunits in the actin filaments is visible in all three micrographs. The long pitch actin helix is also visible in *B*, especially when viewed from the bottom. Comparison of *C* and *D* reveals that the various azimuthal positions of the individual S1s are readily identified in the replica. A minority of the heads are attached laterally where their angle relative to the actin filament can be appreciated. Magnification of the micrographs is 200,000.

ble as longitudinal filaments in the micrographs of the replicas.

The replicas were very heterogeneous with both well-preserved areas and other areas with artifacts that occur during both the freezing and replication. The superficial layers were usually well frozen and deep parts poorly frozen. In well-frozen areas there were no ice crystals, and the filaments were evenly distributed and uniform in morphology. In the deep, poorly frozen areas the proteins were crushed between large ice crystals. In marginal areas, the filaments were clumped and irregular in outline. Before replication, the fracture face was etched a small amount to expose filaments.

Ideally, the filaments were partially submerged in the ice at the time of replication (Fig. 4, *B* and *C*), because after extensive etching, many filaments were completely exposed and subject to damage during replication. The deeply etched specimen in Fig. 4 *A* is well preserved, but replication artifacts are common, including the loss of subtle details like the 5.5 nm repeat along the actin filaments or even gross damage where the molecules appeared to have melted together. These freezing and replication artifacts are easily recognized by experienced observers. We analyzed only those parts of the replicas where there was no visible damage arising from freezing or replication.

The actin filaments frozen in the thin-walled copper flow cells (Fig. 4 *A*) were identical in appearance to actin filaments prepared by impact freezing at liquid helium temperatures (Heuser and Cooke, 1983). They were ~9 nm wide and featured a 5.5-nm axial repeat. In favorable specimens, especially where the polymer was stabilized by being partially submerged in ice, both the left-handed genetic helix and the right-handed long pitch helix are preserved (Fig. 4 *B*).

Actin filaments frozen in the presence of S1 were decorated with small bumps (Figs. 4 *C*, 5, and 6). These bumps are S1 because their number depended on the concentration of S1 (Figs. 5 and 6). At low ratios of S1:actin, individual myosin heads were easily distinguished (Figs. 4 *B* and 5, *A* and *B*). Actin filaments saturated with S1 had a rope-like appearance (Figs. 5 *D* and 6

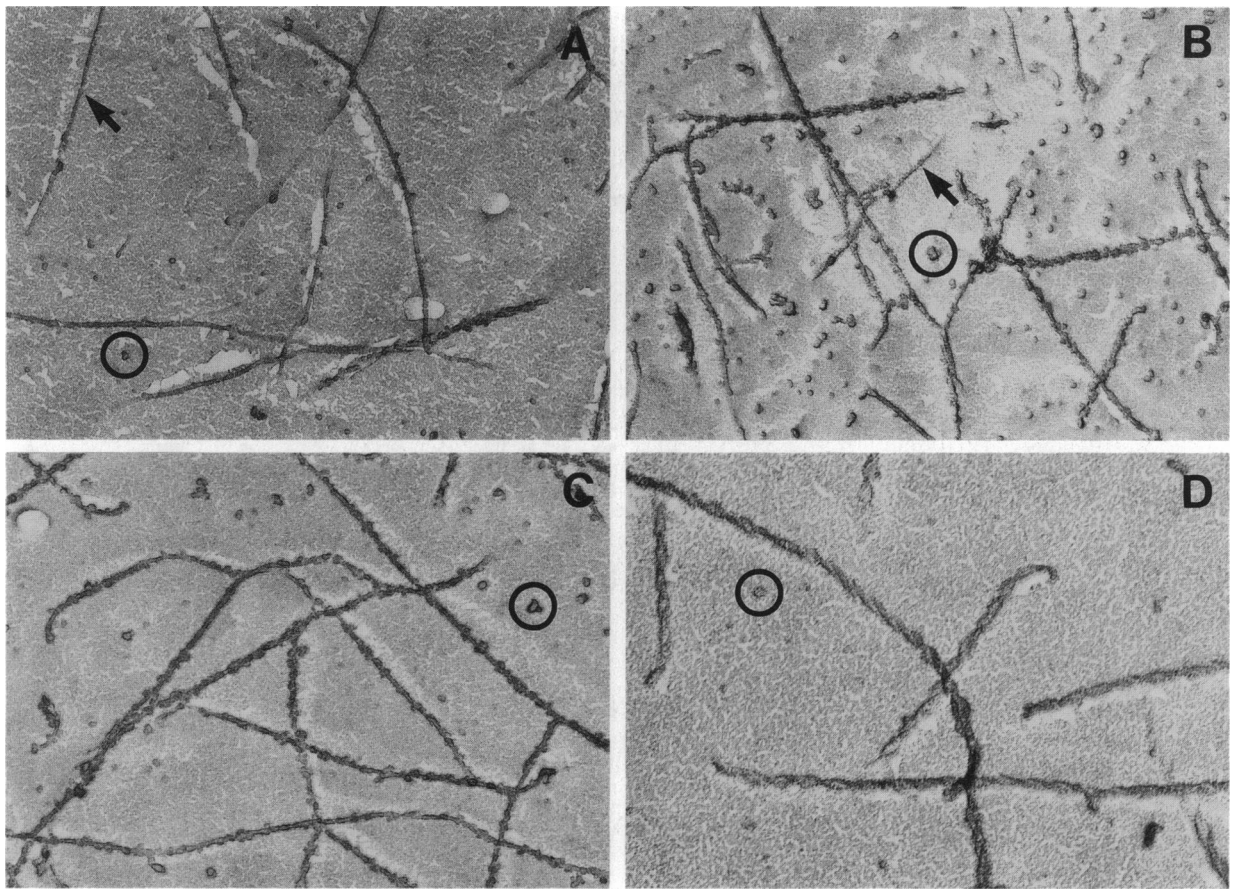


FIGURE 5 Electron micrographs of fields of rapidly frozen rigor complexes of S1 with actin filaments over a range of S1 concentrations. All samples contained 30 μM polymerized actin. The S1 concentrations were (*A* and *B*) 2 μM and (*C* and *D*) 20 μM. Cross sections of actin filaments are circled in each micrograph. Arrows in *A* and *B* indicate lightly decorated filaments. Both of these fields also illustrate more heavily decorated filaments. Magnification, 100,000.

*D*) first described by Heuser and Kirschner (1980). These ropes were 23 nm wide and had an axial repeat of 37 nm.

At substoichiometric ratios of S1 to actin the density and distribution of S1s on individual actin filaments was variable in both the absence (Fig. 5) and presence of ATP (Fig. 6). Many filaments had only a few scattered heads bound, whereas other filaments in the same field were densely decorated (Fig. 5, *A* and *B*). This indicates that binding is cooperative under our conditions.

At high magnification, the replicas of individual myosin heads attached to actin filaments were remarkably similar to three-dimensional reconstructions of S1 made from electron micrographs of negatively stained (Taylor and Amos, 1981; Vibert and Craig, 1982; Toyoshima and Wakabayashi, 1985) and frozen hydrated (Milligan and Flicker, 1987; Milligan et al., 1990) actin filaments saturated with S1. By comparison with the published reconstructions (Fig. 4 *D*), it was possible to judge the azimuthal angle of attachment of these myosin heads in the replicas. Some heads were clearly attached to the upper surface of the filaments and appeared as bright highlights. Others were partially hidden on the back side of the filaments. Less than 10% were attached to the sides of the filaments in positions where they were fully exposed, and their angle of attachment could be measured. We restricted our analysis to these laterally attached myosin heads. The replicated myosin heads projected 9 ± 2 nm (means ± SD) laterally from the edge of the actin filaments. Including the part of the head on the top surface of a replicated filament, the longest dimension of the heads was ~16 nm, the same length measured in reconstructions of heads from electron micrographs of S1 crystals (Winkelman et al., 1991). The long axis of most of these heads clearly made an acute angle with respect to the long axis of the actin filament. These angles are described in detail in the next section.

The morphology of the attached S1s was the same in the absence (Fig. 7) and presence (Fig. 8) of ATP. A sample of 26 rigor heads projected 9.5 ± 2.0 nm beyond the actin filament. A sample of 47 heads frozen 50 ms after mixing with ATP projected 9.5 ± 0.5 nm. Blinded observers could not distinguish a mixture of micrographs. This included the appearance of the ropes that form when actin is saturated with myosin heads (Figs. 5 *D* and 6 *D*). Higher concentrations of S1 than actin were

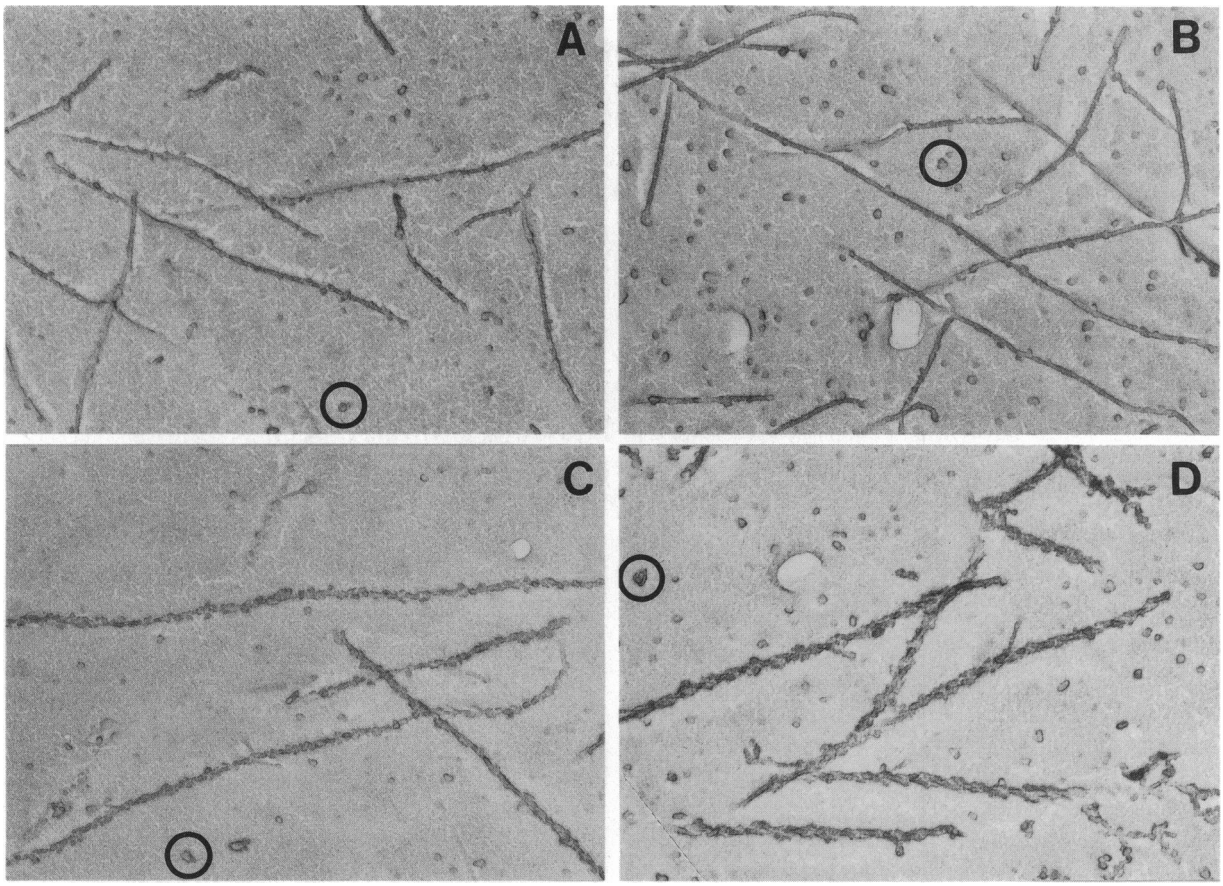


FIGURE 6 Electron micrographs of fields of rapidly frozen S1 intermediates weakly bound to actin filaments in the presence of ATP. All samples contained 30 $\mu$M polymerized actin and 0.25 mM ATP and were frozen 50 ms after mixing. The S1 concentrations were (*A*) 5 $\mu$M, (*B*) 12 $\mu$M, (*C*) 10 $\mu$M, and (*D*) 40 $\mu$M. Cross-sections of actin filaments are circled in each micrograph. Magnification, 100,000.

required to saturate most of the filaments in the presence of ATP, but the diameter, helical repeat, and overall appearance were the same as the rigor complexes in the absence of ATP.

## Quantitative comparison of weakly bound intermediates and rigor complexes

We used measurements of the angle of attachment of S1 to actin to compare weakly bound intermediates with rigor complexes. These measurements were made blind by three of the authors. Although the observers differed in the number of heads that they accepted for measurement, their measurements were otherwise the same in terms of the mean angles, standard deviations, and shapes of the distributions. Consequently, we are confident that the results presented below are unbiased and reproducible.

In scoring the angles of attachment, we assumed for each filament that the majority of the heads were bound at angles between 0 and 90°. This is a reasonable assumption in the case of rigor complexes, given the previous three-dimensional reconstructions of negatively stained specimens. We attempted to confirm the validity of this assumption for the weakly bound intermediates by mixing S1 with ATP and hybrid filaments consisting of bare actin filaments grown from short segments of actin filaments saturated with covalently bound S1 (Tseng et al., 1984). However, it was impossible to collect a statistically significant sample of attachment angles for weakly bound S1s attached to bare filaments adjacent to the polarity markers.

In both rigor and in the presence of ATP, a majority of the S1s attached to actin at angles between 30 and 60° (Fig. 9). The rigor samples were made in several ways. Some were made by mixing S1 with actin filaments depleted of ATP by dialysis. Others were made by mixing S1 with actin filaments in ATP and waiting a time well beyond the hydrolysis of the ATP and the dissociation of products as judged by stopped-flow light scattering measurements made in parallel. The results were equivalent. The weakly bound intermediates were captured by mixing S1 with actin in ATP and freezing during the period of steady-state ATP hydrolysis observed in parallel stopped-flow light scattering experiments. Samples frozen 1, 50, and 250 ms after injection of the mixture into the flow cell gave the same results. Most of the above

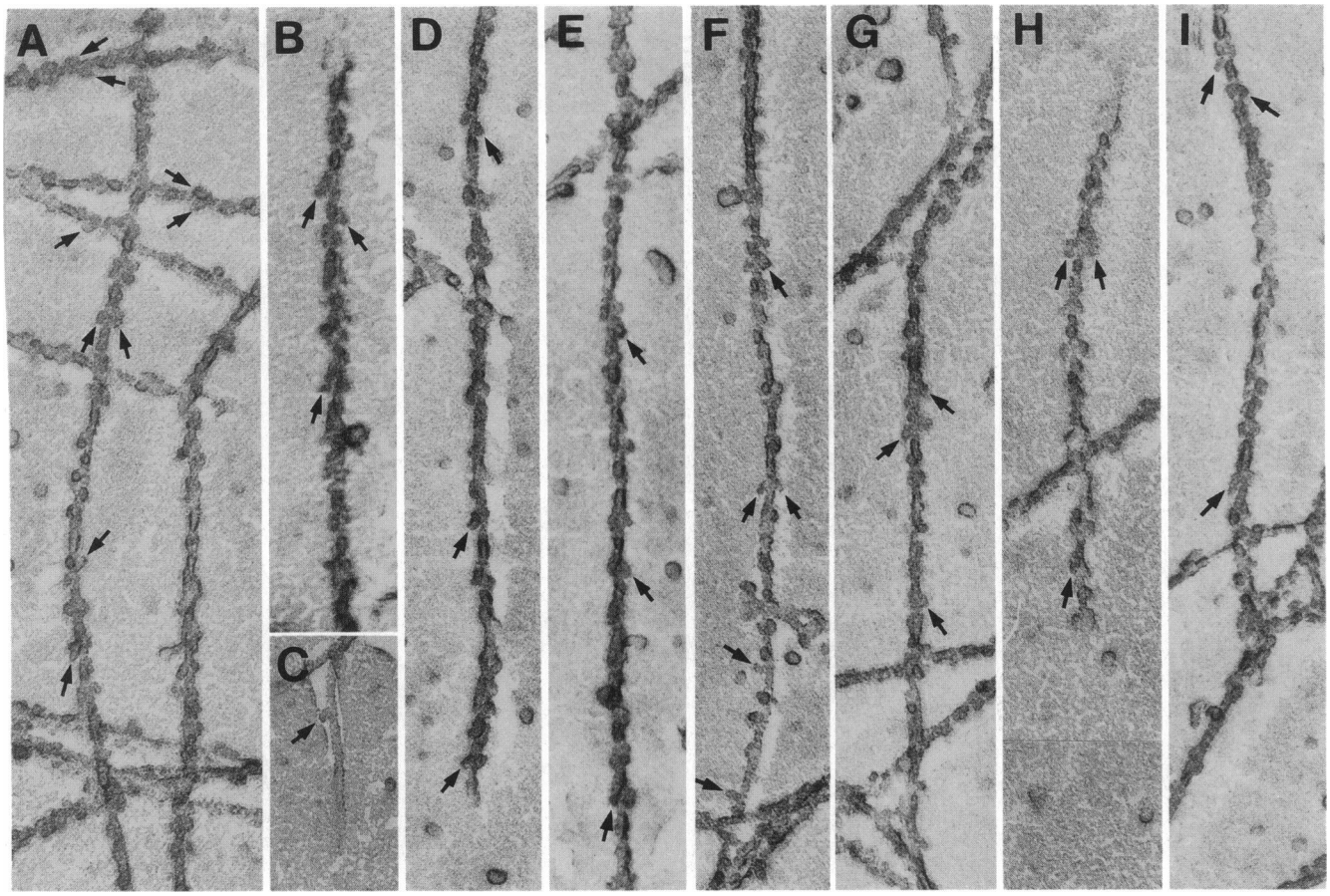


FIGURE 7 Electron micrographs of individual rapidly frozen actin filaments with rigor complexes of S1. The samples contained 30 μM actin and either 2 μM S1 (*C, D, E,* and *I*), 5 μM (*B*) or 20 μM S1 (*A, E, F, G,* and *H*). Arrows indicate the angle of attachment of a few of the myosin heads bound to the actin filaments. Magnification, 200,000.

experiments were with chymotryptic S1, but similar results were obtained in seven experiments consisting of 40 freeze-fracture runs with papain S1.

## Observations on chemically cross-linked acto-S1

We confirmed the observations of Craig et al. (1985) on negatively stained specimens that ATP causes disordering of S1 chemically cross-linked to actin filaments (Figs. 10 *B* and 11 *E*). In the absence of ATP the actin filaments were decorated with scattered but uniformly oriented myosin heads attached at a mean angle of 50° (Figs. 10 *A* and 11 *A*). In the presence of ATP the heads were obviously disordered (Fig. 10 *B*) and the distribution of attachment angles was much broader (Fig. 11 *E*). Under the conditions that these specimens were prepared for electron microscopy, the ATPase was 21 $s^{-1}$, very similar to the $V_{max}$ measured with uncross-linked S1 and actin.

After rapid freezing and replication of chemically cross-linked acto-S1, rigor samples without ATP had relatively uniform myosin heads (Fig. 10, *C–E* and 11, *B–D*), but samples with ATP were less uniform (Fig. 10, *F–I*). In ATP there was a broad distribution of attachment angles, but the sample was skewed strongly toward values between 20 and 60° (Fig. 11 *F*), i.e., with a majority of the heads oriented toward the pointed end. The difference between samples with and without ATP was not as obvious in the quantitation of frozen samples as in the negatively stained specimens.

Compared with negative staining where the full length of each filament is observed, only short segments of each actin filament can be evaluated in replicas. This leads to ambiguity in assigning the polarity of the filaments since relatively few heads can be measured in many cases. Inclusion of filaments with few assigned heads strongly biases the distribution, because of the "majority toward the pointed end" method used to assign the polarity of the filaments. With small numbers of randomly oriented heads, the polarity assigned to a filament is frequently backward and its heads are scored incorrectly in the 0–90° quadrant, accounting for the large fraction of heads with these angles. By eliminating from the analysis the filaments with few attached heads (≤3, ≤5, or ≤9 shown in Fig. 11, *F–H*), the assigned distribution of at-

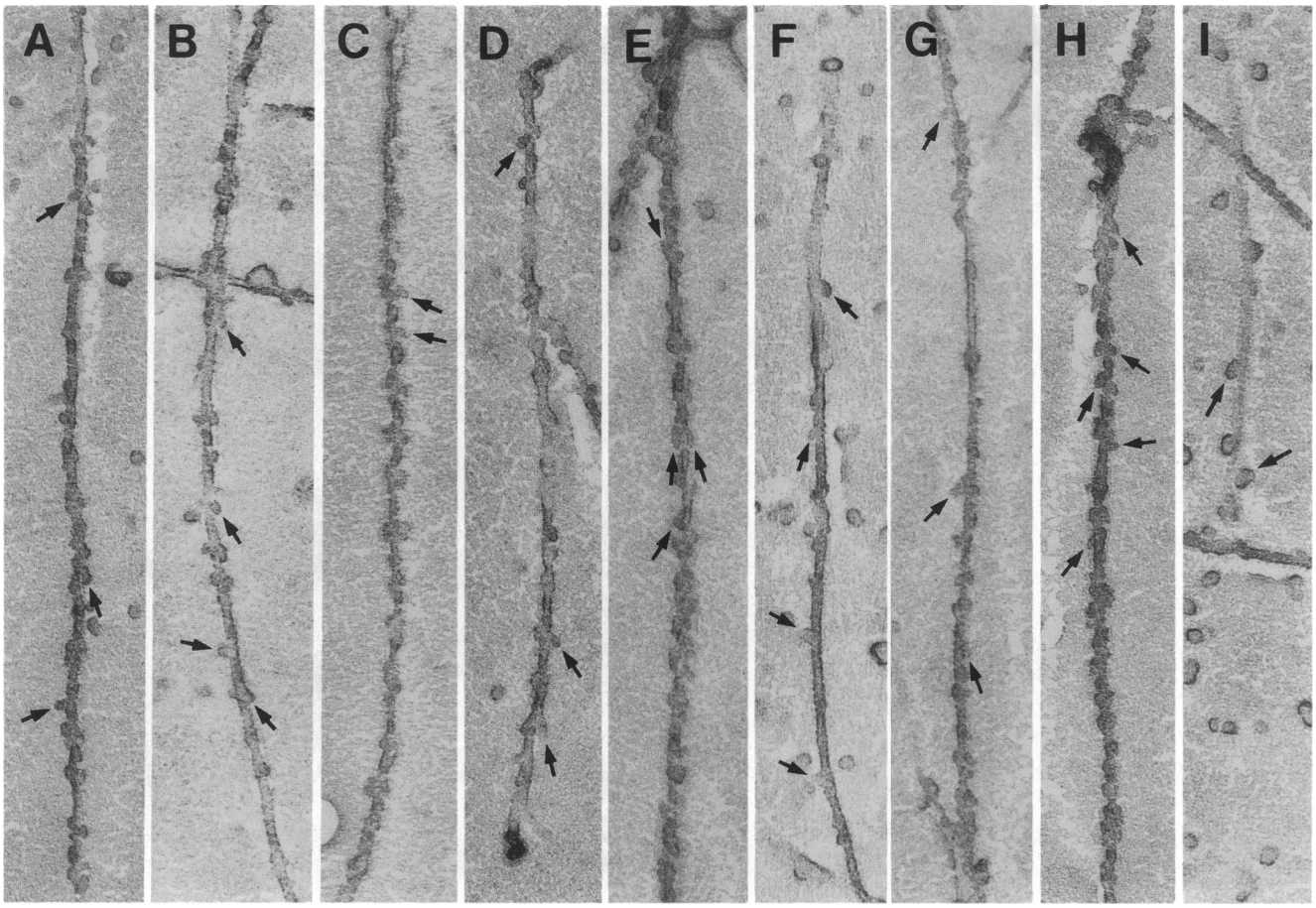


FIGURE 8 Electron micrographs of individual actin filaments with weakly bound S1 intermediates rapidly frozen 50 ms after mixing with ATP. The samples contained 30 $\mu$M actin and either 5 $\mu$M S1 (*A, B, D, E, G,* and *H*), 10 $\mu$M S1 (*C*), or 12 $\mu$M S1 (*F* and *I*). Arrows indicate the angle of attachment of a few of the myosin heads bound to the actin filaments. Magnification, 200,000.

tachment angles approached that predicted for a random distribution, but the distribution was still skewed toward the pointed end.

To establish whether distributions of attachment angles in Fig. 11 are really random or whether our observed skew toward 45° is due to a real tendency of the heads to point in one direction, we used probability theory to calculate (as described in Materials and Methods) the distribution of orientations expected when we scored the polarity of a modest number of heads on a finite number filaments. These calculations showed that for any underlying tendency of the heads to point in one direction ($\omega$), the observed mean angle of attachment is a function of the number of heads per filament, whereas the 95% confidence limit of the spread in the observations is a function of the number of filaments scored.

For example, given a sample of filaments with heads truly attached at random angles, the observations will depend on both the number of heads per filament and number of filaments scored as follows. With a large number of random heads, say 40 per filament, there will be no skew in the observed attachment angles scored by our method; >95% of the time a sample of five or more filaments will give an equal number of heads oriented in each direction. On the other hand, for a population of five filaments with only five randomly oriented heads per filament, 95% of the time between 60 and 80% of the heads will be scored by our method as oriented toward the pointed end. For a population 70 filaments with five random heads per filament, 66–72% of the heads will be scored by our method with pointed orientation 95% of the time. In other words, a truly random population will appear to be skewed toward the pointed end simply due to the method used to assign polarity, if the sample observed is limited in size.

In our samples of EDC cross-linked acto-S1 in the presence of ATP, slightly more heads are oriented in the pointed direction (the 0–90° quadrant of the graphs) than expected from the calculated bias introduced by our method to assign polarity. For example, for a sample of 40 filaments each with five randomly oriented heads, 65–72.5% of the heads will be scored as oriented toward the pointed end 95% of the time. For comparison, we observed 76% of heads oriented in the pointed direction in our sample of filaments with at least five heads per filament. For a sample of 20 filaments with nine random

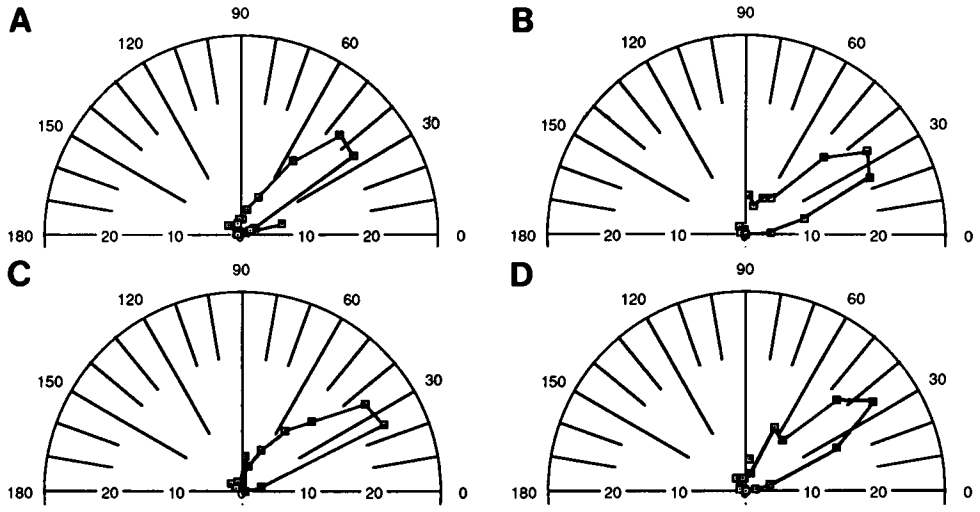


FIGURE 9 Graphs of the distribution of angles of attachment of S1 to actin filaments in the absence and presence of ATP. The data scored separately by two the authors are presented in polar coordinates with the angle representing the angle of attachment and the radius representing the frequency. (*A*) Rigor complexes measured by TP. (*B*) Rigor complexes measured by PM. (*C*) Intermediates measured by TP. (*D*) Intermediates measured by PM. The samples included the following number of heads: *A*, 249; *B*, 132; *C*, 207; *D*, 212.

heads, the 95% confidence limits are 58–67% scored as oriented toward the pointed end. We observed 71% oriented in the pointed direction in our sample of filaments with at least nine heads.

Based on this comparison of our observations with the results expected from a sample with randomly oriented heads, we conclude that the distribution of attachment angles for cross-linked acto-S1 is nearly random in the presence of ATP, but that there is an underlying tendency for the heads to be oriented toward the pointed end of the filaments. We estimate from the difference in the calculated and observed bias that ~15% of the heads are actually oriented toward the pointed end, and the remaining heads are randomly attached.

## DISCUSSION

### Previous biophysical studies of crossbridge motion

The myosin crossbridge has long been the focus of efforts to understand how ATP hydrolysis produces force and motion during muscle contraction and other forms of cellular motility. Since isolated myosin heads have full ATPase activity (Lowey et al., 1969) and can move actin filaments in an in vitro assay (Toyoshima et al., 1987), most investigators except that the crossbridge motion is generated by the myosin heads and actin, whereas the rest of the myosin molecule plays a supportive role.

Structural studies on the interaction of the myosin heads with actin filaments have been limited by three factors. First, the crossbridges in muscle (Huxley and Brown, 1967) as well as isolated S1 and actin in solution traverse the ATPase cycle asynchronously, so that spectroscopic averaging techniques record a blurred signal from a large population of molecules (Thomas, 1987). Second, crossbridges in active muscle bind to and dissociate from the actin filaments > 100 times per second, and the actual force-producing step may be even faster (reviewed in Hibbard and Trentham, 1986), so that the key intermediates are present in low concentrations and are difficult to capture in time. The concept of rapid transitions between bound and free myosin is generally accepted for the weakly bound AMT and AMDP intermediates but also may apply to the force producing intermediates (Brenner, 1991; Lombardi et al., 1992). Third, although important progress is being made on the structure of the myosin head by structural analysis of three-dimensional crystals (Winkelman et al., 1985, 1991) and other methods (reviewed by Vibert and Cohen, 1988), no structural information at atomic resolution was available at the time of this study. More than anything else, the forthcoming high resolution structure of the myosin head from x-ray crystallography will clarify our thinking about the mechanism of force transduction.

These limitations of structural studies of contracting muscle have been circumvented to some extent by using x-ray diffraction to follow changes during the recovery of tension after small, rapid shortening steps (Huxley et al., 1982; Irving et al., 1992). The step more or less synchronizes the action of the heads during the recovery of force, and there is a good correlation between the time courses of the change in tension and the change in intensity of the 14.5-nm meridional reflection. On the other hand, the observed change in intensity is open to many structural interpretations, so these studies have not resolved the questions about the mechanics of force production.

Most of the recent progress has been in defining the kinetics and thermodynamics of the chemical reactions

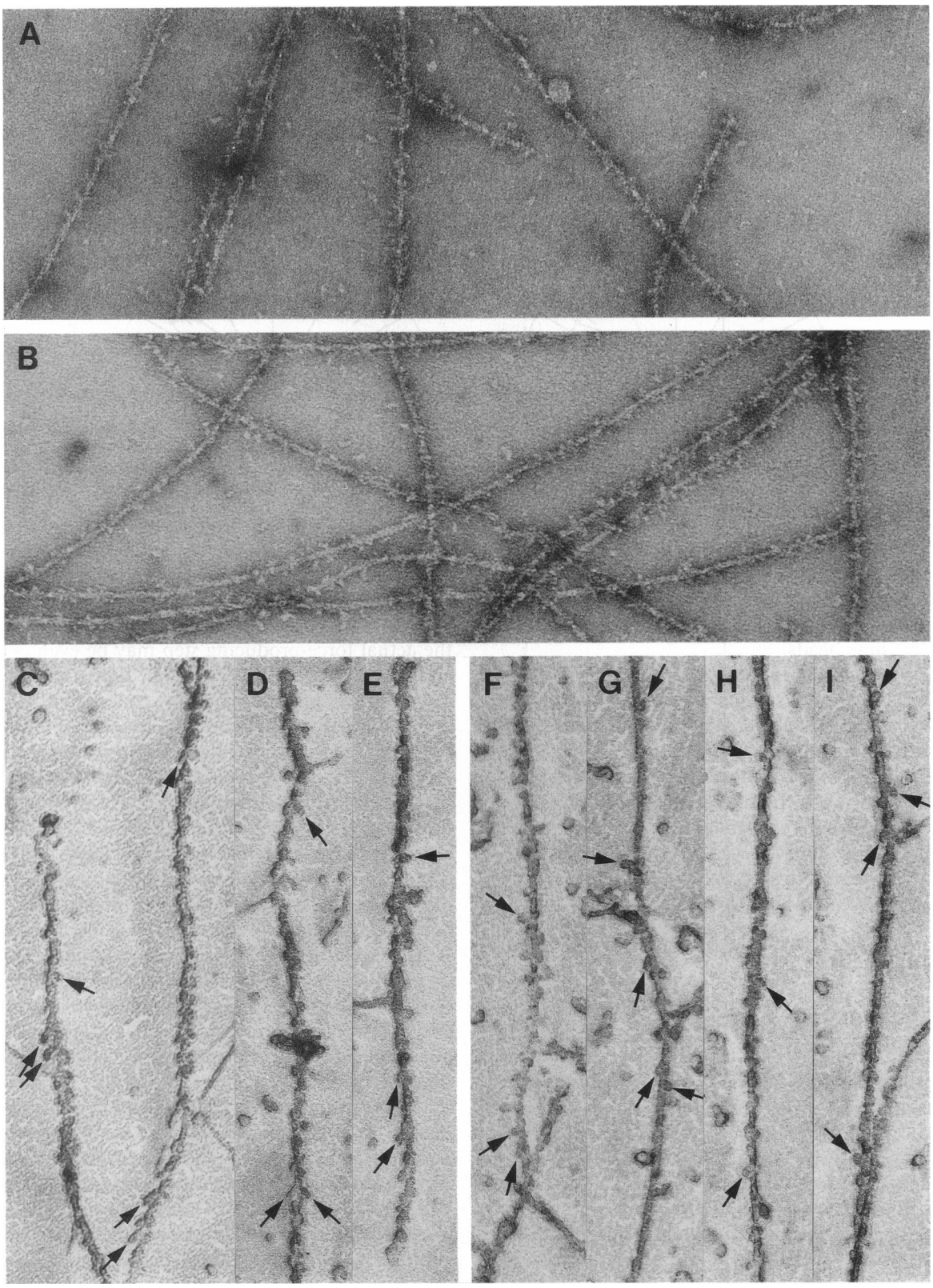


FIGURE 10 Electron micrographs of S1 chemically cross-linked to actin filaments with EDC. (*A*) Negatively stained rigor complexes without ATP. (*B*) Negatively stained in the presence of 0.5 mM ATP. (*C–E*) Replicas of rapidly frozen rigor complexes without ATP. (*F–I*) Replicas of samples rapidly frozen 50 ms after mixing with 0.5 mM ATP. Arrows indicate the angle of attachment of a few of the myosin heads bound to the actin filaments. Magnification, 200,000.

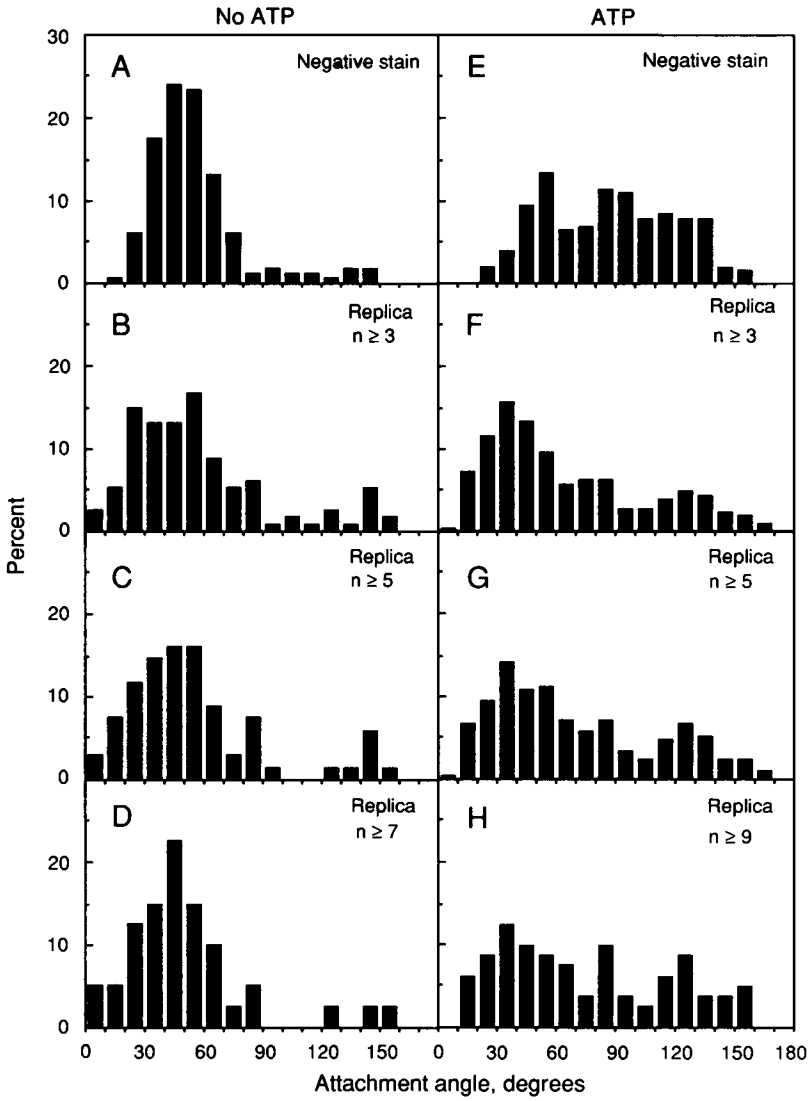


FIGURE 11 Quantitation of S1 attachment angles for the samples of cross-linked acto-S1 illustrated in Fig. 10. (*A–D*) Samples without ATP. (*E–H*) Samples with 0.5 mM ATP. *A* and *E* were prepared by negative staining. Samples *B–D* and *F–H*) were prepared by rapid freezing. For the rapidly frozen samples, filaments with small numbers of scored S1s were excluded as follows. (*B* and *F*) Filaments with ≥3 heads. (*C* and *G*) Filaments with ≥5 heads. (*D*) Filaments with ≥7 heads. (*H*) Filaments with ≥9 heads. The samples included the following numbers of heads: *A*, 167; *B*, 114; *C*, 68; *D*, 40; *E*, 202; *F*, 301; *G*, 213; *H*, 81.

involving myosin, actin, and ATP as summarized in the Introduction. These elegant studies have shown that the energy required for the production of force and motion is provided by binding and hydrolysis of ATP on the myosin head, stored as a conformational change in the MT and MDP intermediates, and released when the products (particularly phosphate) dissociate from AMDP.

Having identified the place in the ATPase cycle (Fig. 1) where motion is produced, one must ask where is the motion in the actin-myosin complex? Conventional crossbridge models assume that the movement of myosin relative to actin is the direct consequence of a major structural rearrangement in the crossbridge during the transition from AMDP to AMD (Huxley and Kress, 1985) or by isomerization of the AMDP complex (Geeves, 1991).

Several independent spectroscopic methods establish the existence of conformational changes during the actomyosin ATPase cycle, but these structural changes have not been linked directly to something as simple as a tilting crossbridge. (*a*) ATP hydrolysis is accompanied by a change in intrinsic fluorescence of the myosin head (Chock et al., 1979). (*b*) A slow first order quenching of the fluorescence of a pyrenyl probe on cysteine 374 of actin follows the second order binding of M or MD to actin filaments (Geeves, 1989; Taylor, 1991). (*c*) A change with similar kinetic constants occurs in the fluorescence of mant-ATP bound to the active site on myosin (Woodward et al., 1991) and is thought to reflect the

same conformational change. (*d*) Fluorescence resonance energy transfer revealed a large (3 nm) difference in the distance between fluorescent probes on actin and the essential myosin light chain for weakly and strongly bound actomyosin complexes (Bhandari et al., 1985; Trayer and Trayer, 1988). The occurrence of parallel changes sensed by probes > 5 nm apart in the acto-S1 complex argues that the isomerization is a global, large-scale change in the complex; however, none of this evidence reveals whether the conformational changes are large enough to produce the motion required by conventional crossbridge models. A comparison of the shape of S1 bound to actin filaments or free in solution by neutron scattering detected no difference (Curmi et al., 1988).

Other spectroscopic studies have sought changes in the orientation of the myosin heads relative to actin filaments during the ATPase cycle. Both fluorescence polarization (Yanagida, 1985) and conventional electron paramagnetic resonance (EPR) probe studies (reviewed Thomas, 1987; Cooke, 1990) have detected differences in the proportions of bound and free myosin heads in relaxed, contracting, and rigor muscle but have not revealed a significant population of novel myosin intermediates, such as the 90° intermediates that are postulated by standard crossbridge models to be bound to actin in active muscle fibers. On the other hand, saturation transfer EPR experiments have revealed a dramatic increase in rapid (microsecond) motions of an EPR probe on myosin heads weakly attached to actin filaments in ATP (Berger et al., 1989). This change in mobility is strong evidence for a difference in the structure of these weakly bound intermediates compared with rigor. The rapid motion is in the myosin head and not the actin filament (Ostap and Thomas, 1991), and its structural basis remains to be elucidated.

## New observations by electron microscopy

The goal of our study has been to identify any large-scale structural changes in the actin-myosin complex that might couple the actomyosin ATPase cycle to the production of force and motion. Given the large size of the myosin head, we felt that the most direct approach to detect the large-scale structural changes postulated by models for contraction would be to obtain electron micrographs of the weakly bound intermediates (AMT and AMDP) for comparison with the well-characterized rigor complex (AM). Such a comparison has the potential to reveal directly any large-scale molecular motion, since the weakly bound intermediates are generally considered to be the preforce-producing intermediates and the rigor complex is considered to be the final force-producing state.

The main result of the present work is that the unloaded, weakly bound myosin S1 intermediates in the actin-myosin ATPase cycle are indistinguishable from tightly bound rigor complexes by electron microscopy. This conclusion is based largely on measured angles of attachment of individual S1 molecules (Figs. 8 and 9) and is supported by the regular appearance of filaments saturated with nucleotide bearing intermediates (Fig. 6 *D*).

## Technical limitations of the present studies

We recognize that the validity of our observations depends on the fidelity with which our methods preserve the protein molecules for observation in the electron microscope. The experiments are reproducible, so we can rule out random artifacts. It is more difficult to prove that none of the steps in the preparation for electron microscopy have introduced consistent, reproducible artifacts. In the following paragraphs, we consider the most likely sources of artifacts. In spite of these potential pitfalls, we believe that the images presented here are reasonable likenesses of the native proteins.

For our approach to work, the samples must be frozen, etched, and replicated without distortion of the shape of the S1 molecules. The extensive damage always present deep in the frozen specimens, more than $\sim 1$ $\mu$m from the inner surface of the copper tube, is a constant reminder that the freezing process is hazardous. The facts that no ice crystals are visible in the areas studied and that the actin and the attached S1 are similar in appearance to these molecules frozen at liquid helium temperatures (Heuser and Cooke, 1983) are reassuring. Once frozen, the proteins are likely to be stable during etching at $-106$°C, since the water bound to the protein will maintain it in frozen state during the sublimation of the surrounding solvent water (Gross, 1987). Nevertheless, drying in a vacuum and replication with platinum can produce rather obvious artifacts in the proteins in parts of these specimens. We used a minimum of etching, hoping that filaments partially submerged in ice would be less subjected to damage, but even this precaution cannot rule out some subtle alteration in the shape of the S1. For example, we cannot rule out that some step in the preparation causes molecules with genuinely different shapes to decay into some common low energy structure. Such a transformation could account for the uniform shapes of both the rigor complexes and weakly bound intermediates. Fortunately, the available information on the kinetics of transitions in crossbridges induced by rapid temperature changes (Davis and Harrington, 1992) suggests that rapid freezing at the rates we used might shift the population of heads into the state immediately before force production, but that other transitions would be too slow to occur during freezing. Therefore, this "artifact" would enrich for the very intermediates that we were seeking.

A second reservation about the work is the low resolution inherent in the replication method. Although metal replication has successfully reproduced molecular de-

tails of a variety of proteins (Heuser, 1983), subtle details in the S1 molecule may have been obscured during replication. Therefore, we are limited in detecting only the type of large conformational changes hypothesized in the conventional crossbridge models with translations of 5–10 nm for myosin relative to actin during each crossbridge cycle.

A third concern is the use of myosin S1. At the outset of this work, there was no evidence that S1 separated from the rest of the myosin molecule could produce force and movement of actin filaments, but the in vitro experiments have proven that S1 is capable of producing both motion (Toyoshima et al., 1987) and force (Kishino and Yanagida, 1988). Nevertheless, the protease digestion used to prepare S1 may have altered some of the properties of the myosin head. For example, chymotrypsin destroys one light chain (Weeds and Taylor, 1975) and may also truncate the heavy chain within the head (Rimm et al., 1989). The absence of the COOH-terminal part of the heavy chain and the light chain, both near the head-tail junction (Vibert and Craig, 1982), may have made it impossible for us to detect structural changes in the distal part of the head during the ATPase cycle. Similar but less extensive results with papain S1 containing both light chains suggest that chymotrypic digestion may not be a problem.

Fourth, we might lose the important intermediates, because the S1 heads have no mechanical load in our experiments. Since the lifetimes of intermediates may depend on strain, some intermediates produced by ATP binding and hydrolysis might decay rapidly without a mechanical load (Vibert and Cohen, 1988; Geeves, 1991).

## Previous studies of the intermediates in the actomyosin cycle by electron microscopy

Owing to the low affinity of the AMT and AMDP intermediates for actin filaments, the pioneering efforts by Craig et al. (1985) and Applegate and Flicker (1987) to visualize these structures by electron microscopy used S1 covalently bound to actin. Since the S1 cross-linked to actin has ATPase activity equal to the $V_{max}$ of free S1 in the presence of infinite actin (Mornet et al., 1981), these investigators made the reasonable assumption that the cross-linked S1 would be irreversibly associated with actin, not only by the covalent isopeptide bond formed during cross-linking but also by intermolecular bonds with actin. In the presence of ATP, the covalently cross-linked heads were disordered, compared with the regular tilted structure of rigor complexes (Craig et al., 1985; Applegate and Flicker, 1987). The authors suggested that the weakly bound intermediates bind to actin at a range of angles. This interpretation fit with the expectations of some investigators who had equated weak binding with disordered structure, as if rapidly reversible molecular interactions do not necessarily have a defined stereochemistry. (See Huxley and Kress, 1985, for a discussion of this point.)

We have extended the earlier work on cross-linked acto-S1 by quantitative analysis of attachment angles and offer a different interpretation. In the presence of ATP, the cross-linked heads rapidly bind to and dissociate from the actin molecules, just like free S1 in solution. At any given time, 15% of the heads are oriented like rigor complexes, whereas the majority of the cross-linked heads are dissociated from but tethered to the actin by the covalent bonds. Craig et al. (1985) and Applegate and Flicker (1987) originally offered this tethering hypothesis but favored random angles of attachment to account for the disorder. ATP-induced microsecond motions of S1 cross-linked to actin observed by EPR spectroscopy (Svenson and Thomas, 1986) also can be explained by tethering of dissociated myosin heads.

Katayama (1989) concluded from the first published electron micrographs of the weakly bound intermediates in the actomyosin cycle that their structure differs considerably from the rigor complex. As in our work, Katayama used rapid freezing, etching, and rotary shadowing to prepare the specimens for transmission electron microscopy but froze actin immobilized on mica rather than in solution. We used high concentrations of protein in a low ionic strength buffer to obtain reasonable numbers of weakly bound complexes. Katayama used low concentrations of actin and S1 in 75 mM KCl, conditions where >90% of the S1 is dissociated from actin in the presence of ATP. The appearance of the weakly bound heads associated with the actin filaments in Katayama's electron micrographs is clearly different from the appearance of his rigor complexes. Katayama's interpretation was that rigor heads are elongated structures attached at 45° to the filament axis, whereas weakly bound intermediates are short and rounded in shape. Careful inspection of the micrographs in Katayama's article reveals that virtually all of the heads associated with actin filaments in ATP are located between the filament and the underlying mica. Only rare heads are bound to the upper or lateral surfaces of the actin filaments. Since only those heads bound laterally appear elongated in projection, it is not surprising that few of the heads in samples with ATP look like the extended heads seen in rigor by all investigators. We cannot know the shape of the heads under the filaments for comparison with our observations, since they are obscured from view, but their reduced dimensions can be accounted for entirely by being partially hidden.

Menetret et al. (1991) obtained electron micrographs of frozen-hydrated specimens at intervals during the dissociation of S1 from actin filaments by adenylyl imidodiphosphate (AMP-PNP). The S1 dissociated over ~200 ms. At early times in the reaction, 30 ms after the release of AMP-PNP, the nearly fully decorated filaments transiently became wavy before straightening out as the dissociation of the S1 was completed. There was

not an accompanying change in the appearance of the S1 bound to the actin filaments or of the optical diffraction pattern of the partially dissociated filaments. Release of ATP dissociated the S1 too fast to capture the intermediates by their rapid freezing method. We have not observed wavy actin filaments in samples of S1 and ATP (Fig. 6). Trinick and White (1991) have reported in abstract form a variety of S1 conformations in a similar experiment using frozen hydrated acto-S1 in ATP. Since this method of specimen preparation may have some advantages compared with our method, it will be especially important to compare their observations in detail with ours once they are available.

Frado and Craig (1992) used rapid exchange of solutions on the surface of electron microscope grids to prepare mixtures of actin filaments, heavy meromyosin, and ATP by negative staining. Washing without ATP gave heavy meromyosin heads attached to the actin filaments at an angle of ~45°, frequently with the two heads of one heavy meromyosin attached next to each other on a filament. Washing with ATP had three effects. First, most of the heavy meromyosin dissociated from the actin. Second, most of the attached heavy meromyosin had a heterogeneous "fuzzy appearance." Third, pairs of attached heads were rare, so the authors argued that most of the heavy meromyosin was attached by only one of its two heads. The authors state that heavy meromyosin "in the presence of ATP often appeared to attach to actin at angles centered on about 90°, but this was not possible to quantify precisely owing to the shrinking and stretching of the films of stain over the holes in the carbon film." We agree that the disorder is best explained by single heads binding to actin with the detached heads assuming a wide range of configurations relative to the actin filament. In spite of this disorder, many of the heads in their Fig. 2 can be scored with respect to the angle of attachment. Some are attached perpendicular to the filament axis as emphasized by the authors, but there are also filaments with 5 of 6, 8 of 10, 9 of 12, 3 of 5, and 4 of 4 clearly resolved heads pointed in one direction. Therefore, in our view, these results are consistent with our own observations on the polarity of weakly bound intermediates.

Electron micrographs by Tsukita and Yano (1985) of contracting muscle prepared by rapid freezing provide our best view of active crossbridges in situ. In thin sections of freeze-substituted muscle fibers, most of the myosin heads were associated with the actin filaments in both rigor and isometric contraction. The pattern of these heads decorating the actin formed polarized arrowhead shaped complexes in both cases. Individual molecules were not resolved. Our observations on purified actin and S1 are consistent with those of Tsukita and Yano (1985) on rapidly frozen contracting muscle and provide additional details regarding the individual molecules. A similar study has been reported in abstract form by Hirose et al. (1991). They observed crossbridges in a variety of conformations in contracting muscle, a result different from Tsukita and Yano.

## Interpretation

Our observation that weakly bound intermediates and rigor complexes are indistinguishable at the level of resolution preserved in freeze-fracture replicas agrees well with the growing spectroscopic evidence that subtle rather than large-scale structural changes accompany the production of motion by actomyosin crossbridges. This conclusion is also, in our view, consistent with the earlier electron microscopic studies, although previous authors have stressed different interpretations. It is less clear how our results should be reconciled with the microsecond motion observed in the weakly bound intermediates (Berger et al., 1989).

The simplest interpretation of our observations is that the myosin heads do not tilt on the surface of the actin during the ATPase cycle. If correct, this rules out the popular tilting crossbridge model found in most textbooks. On the other hand, we are not certain about the polarity of the weakly bound intermediates relative to the actin filament. Thus, it is possible that the weakly bound heads are uniformly oriented toward the barbed end rather than the pointed end, i.e., they are backward from rigor. This would provide a 90° tilt during the transition from AMDP to AMD consistent with conventional crossbridge models. Our efforts to establish absolute polarity of these intermediates were inconclusive, so we believe that it is safer to assume that both rigor and intermediate complexes have the same polarity. One could also argue that AMT (largely observed here) and AMDP have different structures and that if one could observe a pure population of AMDP, then one might see an attachment angle closer to 90°. This can be explored in the future with experiments at higher temperatures where the initial burst is larger.

Taking the uniformity of S1 attachment angles at face value, one must look elsewhere for the molecular motion produced by actin and myosin. One idea is that the myosin heads slide along the actin filament interacting with multiple actin subunits during one cycle of ATP hydrolysis (Harada et al., 1990; Vale and Oosawa, 1990). In these models ATP hydrolysis is used to bias the thermal motion of the heads without the complex of myosin and actin necessarily undergoing large-scale changes in structure. This mechanism has no preconceptions about the shape of the myosin-actin complex at any point in the cycle. Our data are consistent with such a model.

Another idea is that individual myosin heads can produce force more than once per ATPase cycle by interacting with multiple actins (Brenner, 1991; Lombardi et al., 1992). Each of these events might involve relatively small displacements and thus require a small structural change in myosin consistent with our observations and the probe studies. On the other hand, Irving et al. (1992) have modeled the changes in the x-ray patterns during

recovery from step shortening with a standard 90–45° tilt of the whole crossbridge relative to the actin filament. Alternate interpretations are, of course, possible given the limited data.

We favor an alternate mechanism with the large domain of the head more or less fixed to actin and the motion produced by a large structural change in or between the smaller domains near the head-tail junction as suggested by Huxley and Kress (1985), Tokunaga et al. (1987), and Winkelmann et al. (1991). These distal domains containing the light chains are an attractive site for such a bend. First, they are lateral to the relatively immobile ATP binding site observed by fluorescence and EPR spectroscopy. Second, this region near the head-tail junction may be more mobile than the rest of the head, since it has been difficult to image in this and other (Milligan and Flicker, 1987; Tokunaga et al., 1987) electron microscopic studies of the S1-actin complex. Poor preservation of this part of the head compared with the bulky part attached to the actin could easily explain our inability to observe a change in molecular shape. Cooke (1990) reports preliminary evidence for very rapid mobility of light chains in this part of the heads in active muscle. Third, a change in the spacing between actin and a fluorescent probe on the light chain is the only evidence available for large-scale structural changes in the head during the ATPase cycle (Bhandari et al., 1985; Trayer and Trayer, 1988). Such a motion near the head-tail junction may be difficult to detect in replicas, since the head actually wraps around the actin filament (Moore et al., 1970; Taylor and Amos, 1981; Vibert and Craig, 1982; Toyoshima and Wakabayashi, 1985; Milligan and Flicker, 1987; Tokunaga et al., 1987; Milligan et al., 1990) rather than projecting radially. Consequently, the more massive proximal part of the head dominates the appearance of the head when viewed in projection after metal coating. Fourth, a comparison of the structure of two types of crossbridges in rigor insect muscle provides further evidence that the distal part of the head is more flexible than the bulky domain associated with the actin filament (Taylor et al., 1989).

This work was initiated by T. D. Pollard, A. G. Weeds, and Hugh E. Huxley at the Medical Research Council Laboratory of Molecular Biology, Cambridge, UK. We are indebted to Mr. Chris Rayburn of the Laboratory of Molecular Biology for constructing the stopped-flow spectrophotometer and the stopped-flow/rapid-freeze machine. Robert Bell and Katie Pollard helped with quantitation of the data. We thank Drs. Edwin Taylor and Ron Vale for their comments on the manuscript.

This work was supported by National Institutes of Health (NIH) research grant GM-26132 to T. D. Pollard, grants from the American Heart Association to D. Bhandari and H. Zot, a grant from the Muscular Dystrophy Association of America to T. D. Pollard, a Guggenheim Fellowship to T. D. Pollard, an NIH MSTP (GM-07309) fellowship to D. Wachsstock, and the Medical Research Council of Great Britain.

*Received for publication 24 July 1992 and in final form 6 October, 1992.*

*Note added in proof:* Readers will be interested in new evidence for interdomain movement in the myosin head obtained by x-ray scattering (Wakabayashi et al. 1992).

## REFERENCES

Applegate, D., and P. Flicker. 1987. New states of actomyosin. *J. Biol. Chem.* 262:6856–6863.

Berger, C. L., E. C. Svensson, and D. D. Thomas. 1989. Photolysis of a photolabile precursor of ATP (caged ATP) induces microsecond rotational motion of myosin heads bound to actin. *Proc. Natl. Acad. Sci. USA.* 86:8753–8757.

Bhandari, D. G., H. R. Trayer, and I. P. Trayer. 1985. Resonance energy transfer evidence for two attached states of the actomyosin complex. *FEBS (Fed. Eur. Biochem. Soc.) Lett.* 187:160–166.

Brenner, B. 1991. Rapid dissociation and reassociation of actomyosin cross-bridges during force generation: a newly observed facet of cross-bridge actin in muscle. *Proc. Natl. Acad. Sci. USA.* 88:10490–10494.

Chock, S. P., P. B. Chock, and E. Eisenberg. 1979. The mechanism of the skeletal muscle myosin ATPase. II. Relationship between the fluorescence enhancement induced by ATP and the initial phosphate burst. *J. Biol. Chem.* 254:3236–3243.

Cooke, R. 1990. Force generation in muscle. *Curr. Opin. Cell Biol.* 2:62–66.

Craig, R., L. E. Greene, and E. Eisenberg. 1985. Structure of the actin myosin complex in the presence of ATP. *Proc. Natl. Acad. Sci. USA.* 82:3247–3251.

Curmi, P. M. G., D. B. Stone, D. K. Schneider, J. A. Spudich, and R. A. Mendelson. 1988. Comparison of the structure of myosin subfragment-1 bound to actin and free in solution. A neutron scattering study using actin made "invisible" by deuteration. *J. Mol. Biol.* 203:781–798.

Davis, J. S., and W. F. Harrington. 1992. Kinetic and physical characterization of force generation in muscle: a laser temperature-jump and length-jump study on activated and contracting rigor fibers. *In* Mechanism of Myofilament Sliding in Muscle. H. Sugi and G. H. Pollack, editors. Plenum Publishers, New York. In press.

Eisenberg, E., and C. Moos. 1968. The adenosine triphosphatase activity of acto-heavy meromyosin, a kinetic analysis of actin activation. *Biochemistry.* 7:1486–1489.

Eisenberg, E., and W. W. Kielley. 1974. Troponin-tropomyosin complex. *J. Biol. Chem.* 249:4742–4748.

Frado, L.-L., and R. Craig. 1992. Electron microscopy of the actin-myosin head complex in the presence of ATP. *J. Mol. Biol.* 223:391–397.

Geeves, M. A. 1989. Dynamic interaction between actin and myosin subfragment 1 in the presence of ADP. *Biochemistry.* 28:5864–5871.

Geeves, M. A. 1991. The dynamics of actin and myosin association and the crossbridge model of muscle contraction. *Biochem. J.* 274:1–14.

Gross, H. 1987. *In* Cryotechniques in Biological Electron Microscopy. R. A. Steinbrecht and K. Zierold, editors. Springer-Verlag, Berlin. 205–215.

Harada, Y., K. Sakurada, T. Aoki, D. D. Thomas, and T. Yanagida. 1990. Mechanochemical coupling in actomyosin energy transduction studied by in vitro movement assays. *J. Mol. Biol.* 216:49–68.

Heuser, J. E. 1983. Procedure for freeze-drying molecules adsorbed to mica flakes. *J. Mol. Biol.* 169:155–195.

Heuser, J. E., and M. W. Kirschner. 1980. Filament organization revealed in platinum replicas of freeze-dried cytoskeletons. *J. Cell Biol.* 86:212–234.

Heuser, J. E., and R. Cooke. 1983. Actin-myosin interactions visual-

ized by the quick-freeze, deep-etch replica technique. *J. Mol. Biol.* 169:97–122.

Hibberd, M. G., and D. R. Trentham. 1986. Relationship between chemical and mechanical events during muscle contraction. *Annu. Rev. Biophys.* 15:119–161.

Hirose, K., T. D. Lenart, C. Franzini-Armstrong, and Y. E. Goldman. 1991. Flash and smash: ultrastructure of rabbit muscle fibers rapidly frozen following photolysis of caged ATP. *Biophys. J.* 59:577*a*. (Abstr.)

Huxley, H. E. 1963. Electron microscopic studies of the structure of natural and synthetic protein filaments from striated muscles. *J. Mol. Biol.* 7:281–308.

Huxley, H. E. 1969. The mechanism of muscular contraction. *Science (Wash. DC).* 164:1356–1366.

Huxley, H. E., and W. Brown. 1967. The low-angle x-ray diagram of vertebrate striated muscle and its behavior during contraction and rigor. *J. Mol. Biol.* 30:383–434.

Huxley, H. E., and M. Kress. 1985. Crossbridge behavior during muscle contraction. *J. Muscle Res. Cell Motil.* 6:153–162.

Huxley, H. E., A. R. Faruqi, M. Kress, J. Bordas, and M. H. J. Koch. 1982. Time resolved x-ray diffraction studies of the myosin layer line reflections during muscle contraction. *J. Mol. Biol.* 158:637–684.

Irving, M., V. Lombardi, G. Piazzesi, and M. A. Ferenczi. 1992. Myosin head movements are synchronous with the elementary force-generating process in muscle. *Nature (Lond.).* 357:156–158.

Johnson, K. A. 1986. Rapid kinetic analysis of mechanochemical ATPases. *Methods Enzymol.* 134:677–705.

Katayama, E. 1989. The effects of various nucleotides on the structure of actin-attached myosin subfragment-1 studied by quick-freeze deep-etch electron microscopy. *J. Biochem.* 106:751–770.

Kielley, W. W., and W. F. Harrington. 1959. A model for the myosin molecule. *Biochim. Biophys. Acta.* 41:401–421.

Kishino, A., and T. Yanagida. 1988. Force measurements by micromanipulation of a single actin filament by glass needles. *Nature (Lond.).* 334:74–76.

Kopstad, G., and A. Elgsaeter. 1982. Theoretical analysis of specimen cooling rate during impact freezing and liquid-jet freezing of freeze-etch specimens. *Biophys. J.* 40:163–170.

Lombardi, V., G. Piazzesi, and M. Linari. 1992. Rapid regeneration of the actin-myosin power stroke in contracting muscle. *Nature (Lond.).* 355:638–641.

Lowey, S., H. S. Slayter, A. Weeds, and H. Baker. 1969. Substructure of the myosin molecule. I. Subfragments of myosin produced by enzymatic digestion. *J. Mol. Biol.* 42:1–29.

Lymn, R. W., and E. W. Taylor. 1971. Mechanism of adenosine triphosphate hydrolysis by actomyosin. *Biochemistry.* 10:4617–4623.

Menetret, J.-F., W. Hofmann, R. R. Schroeder, G. Rapp, and R. S. Goody. 1991. Time-resolved cryo-electron microscopic study of the dissociation of actomyosin induced by the photolysis of photolabile nucleotides. *J. Mol. Biol.* 219:139–144.

Milligan, R. A., and P. F. Flicker. 1987. Structure relationship of actin, myosin and tropomyosin revealed by cryo-electron microscopy. *J. Cell Biol.* 105:29–39.

Milligan, R. A., M. Whittaker, and D. Safer. 1990. Molecular structure of F-actin and location of surface binding sites. *Nature (Lond.).* 348:217–221.

Moore, P. B., H. E. Huxley, and D. J. DeRosier. 1970. Three-dimensional reconstruction of F-actin, thin filaments and decorated thin filaments. *J. Mol. Biol.* 279–295.

Mornet, D., R. Bertrand, P. Pantel, E. Audemard, and R. Kassab. 1981. Structure of the actin-myosin interface. *Nature (Lond.).* 292:301–306.

Ostap, E. M., and D. D. Thomas. 1991. Rotational dynamics of spin-labeled F-actin during activation of myosin S1 ATPase using caged ATP. *Biophys. J.* 59:1235–1241.

Pollard, T. D., and E. D. Korn. 1973. *Acanthamoeba* myosin. I. Isolation from *Acanthamoeba castellanii* of an enzyme similar to muscle myosin. *J. Biol. Chem.* 248:4682–4690.

Pollard, T. D., P. Maupin, J. Sinard, and H. E. Huxley. 1990. A stopped-flow rapid-freezing machine with millisecond time resolution to prepare intermediates in biochemical reactions for electron-microscopy. *J. Electron Microsc. Technique.* 16:160–166.

Rimm, D. L., J. Sinard, and T. D. Pollard. 1989. Location of the head tail junction of myosin. *J. Cell Biol.* 108:1783–1789.

Sinard, J. H., and T. D. Pollard. 1990. *Acanthamoeba* myosin-II minifilaments assemble on a millisecond time scale with rate constants greater than those expected for a diffusion limited reaction. *J. Biol. Chem.* 265:3654–3660.

Stein, L. A., P. B. Chock, and E. Eisenberg. 1984. The rate-limiting step in the actomyosin ATPase cycle. *Biochemistry.* 23:1555–1563.

Svensson, E. C., and D. D. Thomas. 1986. ATP induces microsecond rotational motions of myosin heads cross-linked to actin. *Biophys. J.* 50:999–1002.

Taylor, E. W. 1991. Kinetic studies on the association and dissociation of myosin subfragment 1 and actin. *J. Biol. Chem.* 266:294–302.

Taylor, E. W. 1992. Mechanism and energetics of actomyosin ATPase. *In* The Heart and Cardiovascular System. 2nd ed. H. A. Fozzard, editor. Raven Press, New York. 1281–1293.

Taylor, K. A., and L. A. Amos. 1981. A new model for the geometry of the binding of myosin crossbridges to muscle thin filaments. *J. Mol. Biol.* 147:297–324.

Taylor, K. A., M. C. Reedy, L. Cordova, and M. K. Reedy. 1989. Three dimensional reconstruction of insect flight muscle. II. The rigor actin layer. *J. Cell Biol.* 109:1103–1123.

Thomas, D. D. 1987. Spectroscopic probes of muscle cross-bridge rotation. *Annu. Rev. Physiol.* 49:691–709.

Tokunaga, M., K. Sutoh, C. Toyoshima, and T. Wakabayashi. 1987. Location of the ATPase site of myosin determined by three-dimensional electron microscopy. *Nature (Lond.).* 329:635–638.

Toyoshima, C., and T. Wakabayashi. 1985. Three-dimensional image analysis of the complex of thin filaments and myosin molecules from skeletal muscle. IV. Reconstitution from minimal- and high-dose images of the actin-tropomyosin-myosin subfragment-1 complex. *J. Biochem. (Tokyo).* 97:219–243.

Toyoshima, Y. Y., S. J. Kron, E. M. McNally, K. R. Niebling, C. Toyoshima, and J. A. Spudich. 1987. Myosin subfragment-1 is sufficient to move actin filaments in vitro. *Nature (Lond.).* 328:536–539.

Trayer, H. R., and I. P. Trayer. 1988. Fluorescence resonance energy transfer within the complex formed by actin and myosin subfragment 1. Comparison between weakly and strongly attached states. *Biochemistry.* 278:5718–5727.

Trinick, J., and H. D. White. 1991. Electron cryo-microscopy of actomyosin-S1 during steady state ATP hydrolysis. *Biophys. J.* 59:410*a*. (Abstr.)

Tseng, P. C.-H., M. S. Runge, J. A. Cooper, R. C. Williams, and T. D. Pollard. 1984. Physical, immunochemical, and functional-properties of *Acanthamoeba* profilin. *J. Cell Biol.* 98:214–221.

Tsukita, S., and M. Yano. 1985. Actomyosin structure in contracting muscle detected by rapid freezing. *Nature (Lond.).* 317:182–184.

Uyeda, T. Q. P., H. M. Warrick, S. J. Kron, and J. A. Spudich. 1991. Quantitized velocities at low myosin densities in an in vitro motility assay. *Nature (Lond.).* 352:307–311.

Vale, R. D., and F. Oosawa. 1990. Protein motors and Maxwell's de-

mons: does mechanochemical transduction involve a thermal ratchet? *Adv. Biophys.* 26:97–134.

Vibert, P., and R. Craig. 1982. Three-dimensional reconstruction of thin filaments decorated with $Ca^{++}$-regulated myosin. *J. Mol. Biol.* 157:299–319.

Vibert, P., and C. Cohen. 1988. Domains, motions and regulation in the myosin head. *J. Muscle Res. Cell Motil.* 9:296–305.

Wakabayashi, K., M. Tokunaga, I. Kohno, Y. Sugimoto, T. Hamanaka, Y. Takezawa, T. Wakabayashi, and Y. Amemiya. 1992. Small-angle synchroton x-ray scattering reveals distinct shape changes of myosin head during hydrolysis of ATP. *Science (Wash. DC).* 258:443–447.

Weeds, A. G., and R. S. Taylor. 1975. Separation of subfragment-1 isoenzymes from rabbit skeletal muscle myosin. *Nature (Lond.).* 257:54–56.

White, H. D., and E. W. Taylor. 1976. Energetics and mechanism of actomyosin ATPase. *Biochemistry.* 15:5818–5826.

Winkelman, D. A., H. Meekel, and I. Rayment. 1985. Packing analysis of crystalline myosin subfragment-1. Implications for the size and shape of the myosin head. *J. Mol. Biol.* 181:927–936.

Winkelman, D. A., T. S. Baker, and I. Rayment. 1991. Three dimensional structure of myosin subfragment-1 from electron microscopy of sectioned crystals. *J. Cell Biol.* 114:701–713.

Woodward, S. K. A., J. F. Eccleston, and M. A. Geeves. 1991. Kinetics of the interaction of 2′(3′)-O-(N-methylanthraniloyl)-ATP with myosin subfragment-1 and actomyosin subfragment-1: characterization of two acto-S1-ADP complexes. *Biochemistry.* 30:422–530.

Yanagida, T. 1985. Angle of active site of myosin heads in contracting muscle during sudden length changes. *J. Muscle Res. Cell Motil.* 6:43–52.